Design of Penta-Band Omnidirectional Slot Antenna With Slender Columnar Structure

Yue Li, *Member, IEEE*, Zhijun Zhang, *Senior Member, IEEE*, Zhenghe Feng, *Fellow, IEEE*, and Magdy F. Iskander, *Life Fellow, IEEE*

***Abstract*—In this paper, we have proposed a co-located and folded slots antenna for multiband applications. The proposed antenna consists of three radiating slots, arranged on a compact square columnar structure. By properly tuning the dimensions and the positions of the co-located slots, the proposed antenna operates in penta-band, including DCS, PCS, UMTS, 2.5-GHz, and 3.5-GHz WiMAX bands. Additionally, omnidirectional radiation patterns are provided in the azimuthal plane for all the operating bands. The overall volume of the proposed square columnar antenna is only $50 \times 10 \times 10$ mm^3, which is suited for volume-limited systems. A prototype of the proposed antenna is fabricated and tested, to validate the design idea. The measured data, including S parameter, radiation pattern, and gain, agree well with the simulation results.**

***Index Terms*—Antenna radiation patterns, multifrequency antenna, slot antennas.**

I. Introduction

ANTENNA designs with multiple operating bands and omnidirectional radiation patterns are widely studied and adopted in modern wireless communication system, especially for the portable base stations and access points. By using the multiband antennas, more wireless services can be integrated to a single system. And the omnidirectional radiation patterns in the azimuthal plane are also in demand for the large area coverage. Due to these reasons, numerous antenna researchers and engineers are working on this topic.

In recent publications, different antenna design methods are adopted to achieve omnidirectional radiation patterns in the multiple operating bands. First, the monopole antenna with a ground is an acceptable candidate [1]–[10], with the intrinsic omnidirectional radiation pattern in the azimuthal plane. Multiple bands can be achieved by adopting multiple branches with different electrical lengths [1], [2], and parasitical loading [3]–[5] tuning the basic and higher modes. The ultra-wide band (UWB) concept is also used on monopole for multiband coverage, with 2-D [6], [7] or 3-D [8]–[10] structures. Second, we can use dipoles with two symmetrical arms to generate the azimuthal omnidirectional radiation patterns [11]–[14]. Due to the symmetrical structures, the dipoles are feasible to be arranged as array to achieve higher gain in the azimuthal plane [14]. Metamaterial is the third method to achieve omnidirectional patterns for multiple bands application. Periodically arranged metallic posts are adopted to build an omnidirectional radiated mode in [15], [16]. Left-handed loadings are integrated with the loops in [17] and the monopoles in [18]. However, the impedance bandwidth of the metamaterial based omnidirectional antenna is needed to be enhanced. Besides these three methods, other feasible designs are also used to achieve the azimuthal omnidirectional radiation patterns [19]–[22]. For example, a dual-band series-fed antenna using continuous transverse stub (CTS) technology is well designed and fabricated in [19]. In the [20], a dual-band Alford loop antenna is designed to achieve horizontally polarized omnidirectional radiation pattern. We also can employ several directional antennas to form the omnidirectional radiation pattern, such as back-to-back arranged Yagi antennas [21] and slot antennas [22]. However, this design strategy makes the overall antenna volume large.

For the volume-limited systems, such as the portable base stations and access points, 3-D structured antenna with compact dimension is preferred more. Compared with planar 2-D structure, 3-D structured antennas have smaller aspect ratio and more compact volume. In the published literatures, wideband monopoles can be folded to 3-D columnar structure for antenna miniaturization [8]–[10]. A planar ground is needed as the other pole for the monopole type antenna. However, in some circumstances, small-volume equipment cannot provide such large planar grounds. For this reason, other types of antennas without extra ground are required.

In this paper, a penta-band omnidirectional radiated antenna without extra ground is proposed. This antenna consists of three folded slots, which are arranged on a square columnar structure. Omnidirectional radiation patterns are achieved in penta-band, including the digital cellular system (DCS: 1.71–1.88 GHz), the personal communication system (PCS: 1.85–1.99 GHz), the universal mobile telecommunication system (UMTS: 1.92–2.17 GHz), the 2.5-GHz worldwide interoperability for microwave

Manuscript received June 14, 2013; revised August 26, 2013; accepted November 13, 2013. Date of publication November 25, 2013; date of current version January 30, 2014. This work was supported by the National Basic Research Program of China under Contract 2013CB329002, in part by the National High Technology Research and Development Program of China (863 Program) under Contract 2011AA010202, in part by the National Natural Science Foundation of China under Contract 61301001, in part by the National Science and Technology Major Project of the Ministry of Science and Technology of China 2013ZX03003008-002, and in part by the China Postdoctoral Science Foundation funded project 2013M530046.

Y. Li, Z. Zhang, and Z. Feng are with State Key Laboratory on Microwave and Digital Communications, Tsinghua National Laboratory for Information Science and Technology, Department of Electronic Engineering, Tsinghua University, Beijing, 100084, China (e-mail: zjzh@tsinghua.edu.cn).

M. F. Iskander is with HCAC, University of Hawaii at Manoa, Honolulu, HI 96822 USA (e-mail: iskander@spectra.eng.hawaii.edu).

Color versions of one or more of the figures in this paper are available online at http://ieeexplore.ieee.org.

Digital Object Identifier 10.1109/TAP.2013.2292517

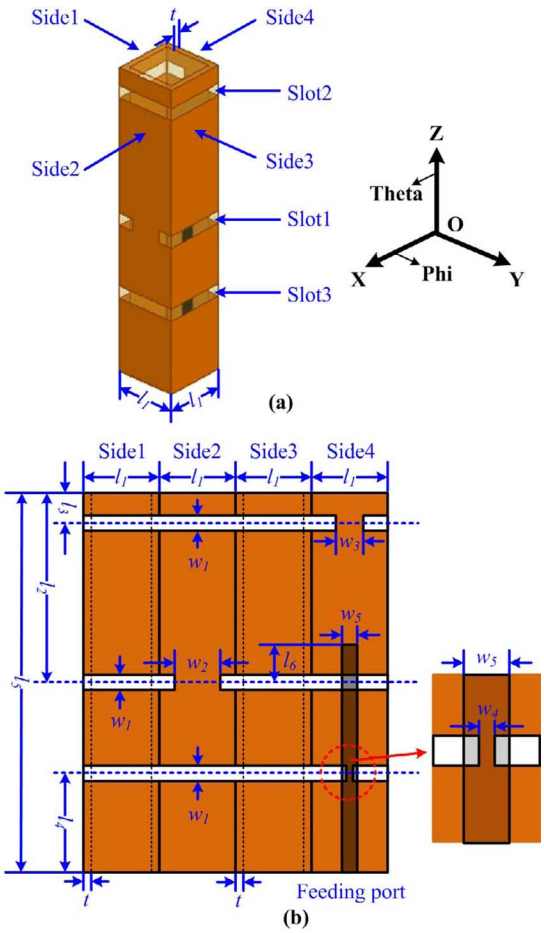

Fig. 1. Geometry and dimensions of the proposed antenna: (a) 3-D view; (b) expanded view.

access (WiMAX: 2.5–2.69 GHz), and 3.5-GHz WiMAX (3.4–3.69 GHz). The overall volume of the proposed antenna is only $50 \times 10 \times 10$ mm^3 ($0.285\lambda_0 \times 0.057\lambda_0 \times 0.057\lambda_0$, λ_0 is the wavelength in free space at 1.71 GHz), which is much smaller than the reference designs. A prototype of the proposed antenna is built to validate the design idea. It is worth mentioning that, the antenna can also be built using double-side soft circuit around a cylinder or a square columnar dielectric die. The operating principle and the optimization method are the same.

The manuscript is arranged as follows. In Section II, the working principle and detailed design strategy of the proposed antenna are described and discussed. The fabrication is then described and the results of the measured reflection coefficient, gain, and radiation patterns are shown and discussed in Section III. Conclusions are presented in Section IV.

II. Antenna Design

Fig. 1 shows the geometry and the dimensions of the proposed antenna. As shown in the 3-D view in Fig. 1(a), the proposed antenna is supported by a center-hollowed square columnar substrate. The substrate is made of FR4 ($\varepsilon_r = 4.4, \tan\delta = 0.02$), with thickness $t = 1$ mm. The proposed antenna consists of four sides (named as Side1, Side2, Side3, and Side4), which are marked on Fig. 1(a). There are three slots (named as Slot1, Slot2, and Slot3) cut from the four sides of the proposed antenna, and are also marked on Fig. 1(a). Slot1 is on the middle of the proposed antenna. The expanded view of Side1 to Side4 is shown in Fig. 1(b). The short ends of Slot1 are on Side2. The short ends of Slot2 and Slot3 are on Side4. A 50-Ω open-ended microstrip line is arranged on the inner side of the substrate, expressed using the dark area. The microstrip line is used to feed Slot1 directly, and cross over the short ends of Slot3. Slot1, Slot2, and Slot3 are with the lengths of $l_1 \times 4 - w_2, l_1 \times 4 - w_3, l_1 \times 4 - w_4$, and with the uniform width of w_1. The values of each parameter are optimized by using the Ansoft High-Frequency Structure Simulator (HFSS) software. The detailed values are listed in Table I. The volume of the proposed antenna is $l_5 \times l_1 \times l_1 = 50 \times 10 \times 10$ mm^3.

TABLE I
Detailed Dimensions (Unit: mm)

l_1	l_2	l_3	l_4	l_5	l_6	w_1	w_2	w_3	w_4	w_5	t
10	25	4	13	50	5	2	5	3	0.4	2	1

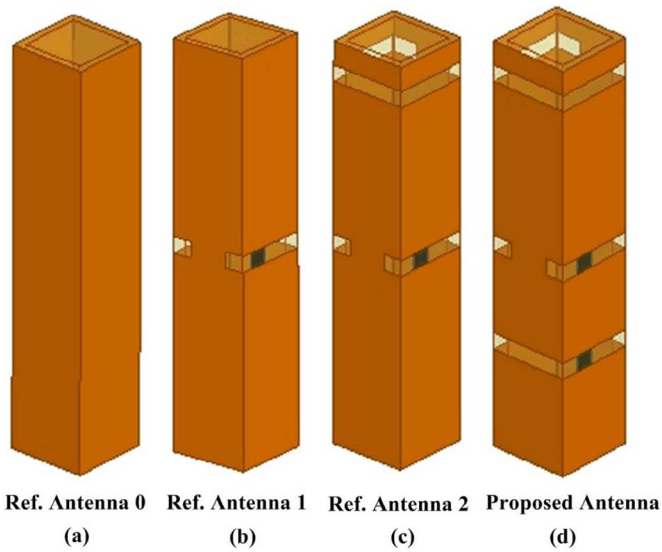

Fig. 2. Referenced antennas and the proposed antenna (a) Ref. Antenna 0, (b) Ref. Antenna 1, (c) Ref. Antenna 2, and (d) Proposed Antenna.

A. Operating Mechanism

In order to discuss the operating mechanism of the proposed antenna, another three reference antennas are utilized and shown in Fig. 2. Ref. Antenna 0, 1, and 2 are with the same dimension as the proposed antenna. Ref. Antenna 0 is with the feeding microstrip line and no slots. Ref. Antenna 1 is only with Slot1 and Ref. Antenna 2 is only with Slot1 and Slot2. The simulated reflection coefficients of four antennas (including the proposed antenna) are illustrated in Fig. 3.

For Ref. antenna 1, the -10-dB bandwidth of the reflection coefficients is from 1.91 GHz to 2.79 GHz, generated by the slot mode. Slot1 is excited by the microstrip line and operates at half wavelength mode. The length of Slot1 determines the working frequency. For Ref. antenna 2, Slot2 is added based on Ref. antenna 1. As shown by the dash curve in Fig. 3, a new resonant frequency appears at approximately 3.3 GHz. This parasitic frequency can be tuned by changing the value of w_3,

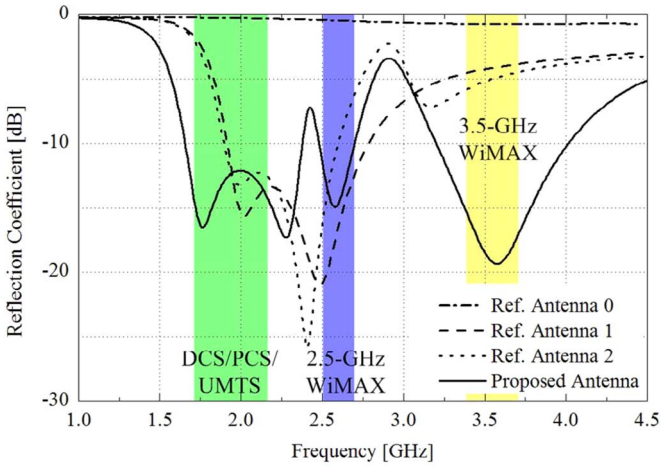

Fig. 3. Simulated S11 of the referenced antennas and the proposed antenna.

but without impedance matching. The −10-dB bandwidth of the reflection coefficients is from 1.89 GHz to 2.59 GHz, succeeded from Ref. antenna 1.

For the proposed antenna, Slot3 is added base on Ref. antenna 2. There are two important functions of Slot3. One is adding another resonant frequency at approximately 2.55 GHz with good impedance matching. This resonant frequency is determined by the length of Slot3. The other one is the defected ground structure (DGS) by adding Slot3. As shown in Fig. 1(b), the short ends of Slot3 are on Side4, with the width w_4 narrower than the width w_5 of the microstrip feeding line. Seen from the port, the input impedance is on longer 50 Ohm. By adding Slot3, the radiating impedance of Slot1 and Slot2 are well matched with enhance bandwidth. Therefore, the simulated −10-dB bandwidth of the reflection coefficients is from 1.66 GHz to 2.37 GHz (lower band), from 2.48 GHz to 2.70 GHz (middle band), and from 3.20 GHz to 4.01 GHz (higher band), covering five bands of DCS (1.71–1.88 GHz), PCS (1.85–1.99 GHz), UMTS (1.92–2.17 GHz), 2.5-GHz WiMAX (2.5–2.69 GHz), and 3.5-GHz WiMAX (3.4–3.69 GHz).

The mechanism of the penta-band operation can be deduced using "adding slot by slot" way as discussed above. However, we cannot conclude directly that each operating band is provided by a certain slot. The triple slots of the proposed antenna are treated as a whole for multiple band operation. In order to examine the working mechanism more clearly, the complex current magnitude distributions of 2 GHz, 2.6 GHz, and 3.5 GHz are shown in Figs. 4, 5, and 6, respectively. The vector electric field distributions in the slots are also illustrated in Fig. 7. We snapped the phase with maximum magnitude of electric field in the slots.

For the lower band, the radiation is mainly contributed by Slot1. As shown in Fig. 4, the current along the edge of Slot1 is the strongest. The slot operates at half wavelength mode with peaks on the short ends and null in the middle, as illustrated in Fig. 7(a). For the middle band shown in Fig. 5, the radiation is mainly contributed by Slot3, with strongest current along the edges of Slot3. The current along Slot2 is also strong. Slot2 also plays an important role for the middle band. From Fig. 7(b), we can see that the resonant fields in Slot2 and Slot3 are not synchronized. For higher band shown in Fig. 6, the radiation is

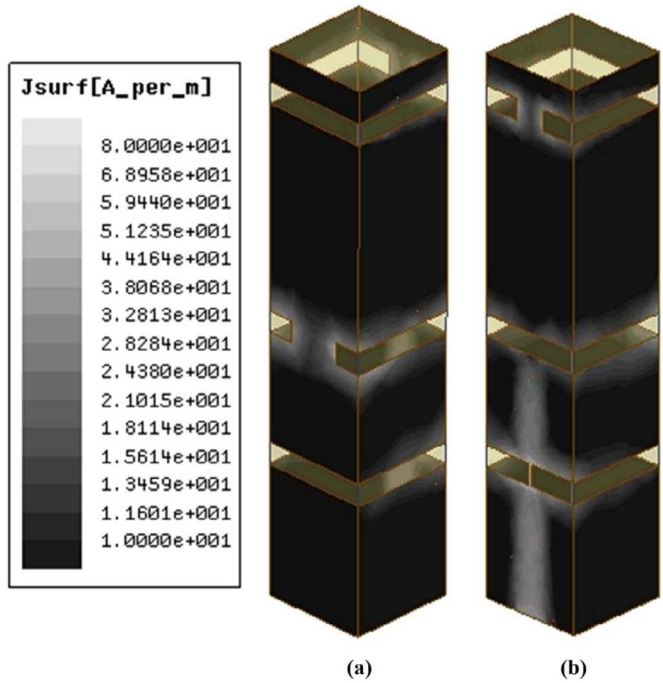

Fig. 4. Complex current magnitude distribution of the proposed antenna at 2 GHz. (a) Side2 and Side3; (b) Side1 and Side4.

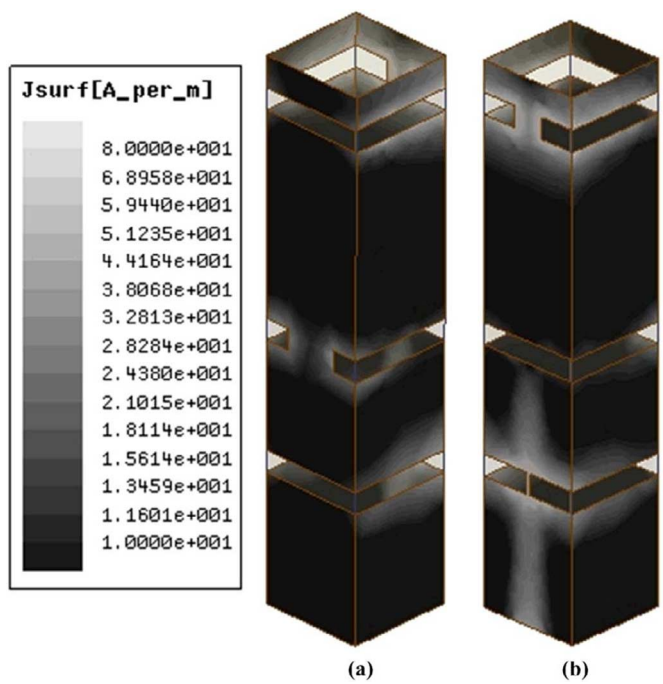

Fig. 5. Complex current magnitude distribution of the proposed antenna at 2.6 GHz. (a) Side2 and Side3; (b) Side1 and Side4.

mainly contributed by Slot2. The currents along the edges of Slot1 and Slot3 are weaker than Slot2. As shown in Fig. 7(c), Slot2 also operates at half wavelength mode. As a more reasonable explanation, Slot2 leads to the creation of a parasitic metal loop ring on the top of the column. As shown in Fig. 6, the currents along the opposite edges of Slot2 are asymmetrical. The current along the upper edge is stronger. The parasitic loop ring also operates at half wavelength mode, which determines the operating frequency. More detailed tuning strategy is introduced in Part C of this section.

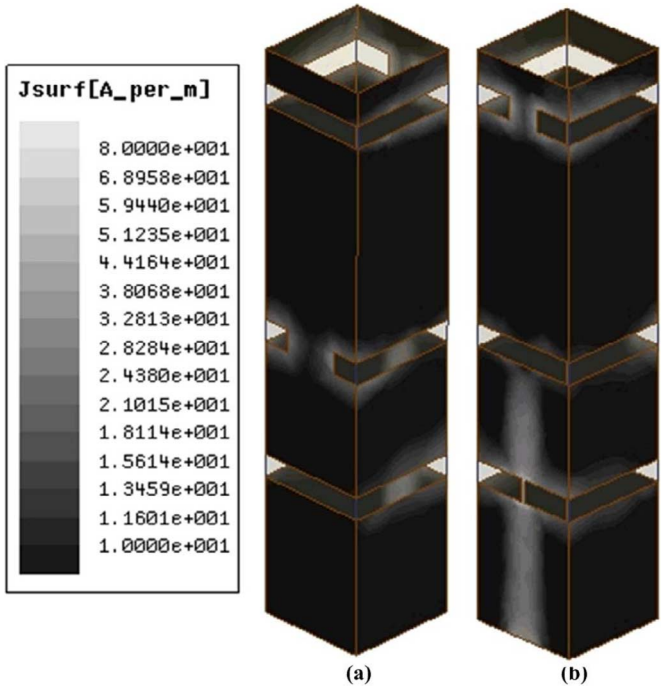

Fig. 6. Complex current magnitude distribution of the proposed antenna at 3.5 GHz. (a) Side2 and Side3; (b) Side1 and Side4.

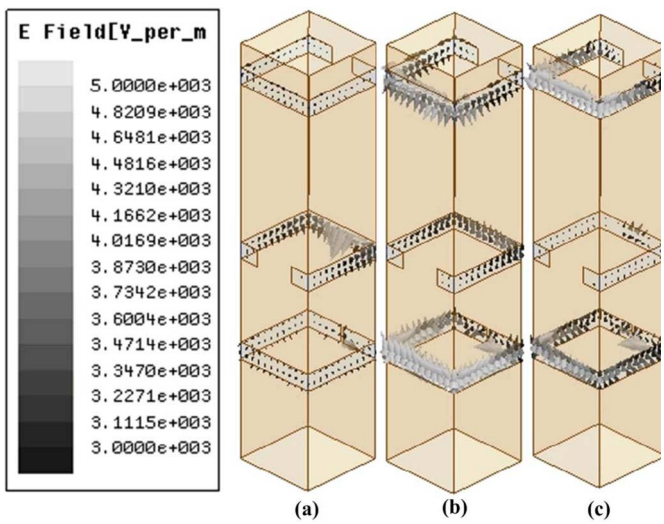

Fig. 7. Vector electric field distribution of the proposed antenna at different operating frequency. (a) 2 GHz, (b) 2.6 GHz, and (3) 3.5 GHz.

B. Omnidirectional Radiation Pattern

Another important characteristic of the proposed antenna is the omnidirectional radiation pattern in the azimuthal plane in all the operating bands. The azimuthal omnidirectional pattern is achieved by folding the slots along the slender columnar structure. By properly tuning the values of w_2, w_3, and w_4, the gain variation between the maximum and the minimum can be controlled. However, as mentioned above, these values are also used for impedance matching. Therefore, there is a tradeoff between the omnidirectional patterns and impedance matching in the parameter optimization.

The simulated radiation patterns at 2 GHz, 2.6 GHz, and 3.5 GHz in the azimuthal plane (XY-plane) are shown in Fig. 8, using the dimensions list in Table I. The gain variations for these

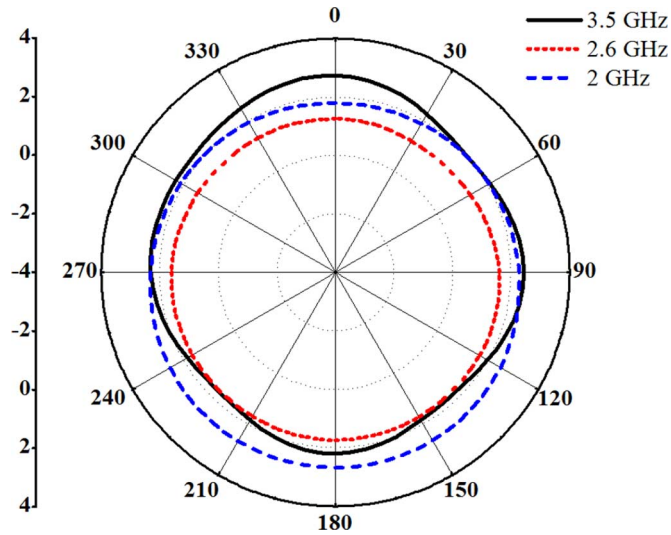

Fig. 8. Simulated radiation pattern of E_θ in the azimuth plane (XY-plane) at the frequencies of 2 GHz, 2.6 GHz and 3.5 GHz. (Unit of left legend: dB).

TABLE II
GAIN VARIATIONS

Frequency	2 GHz	2.6 GHz	3.5 GHz
Value	1.05 dB	0.55 dB	0.89 dB

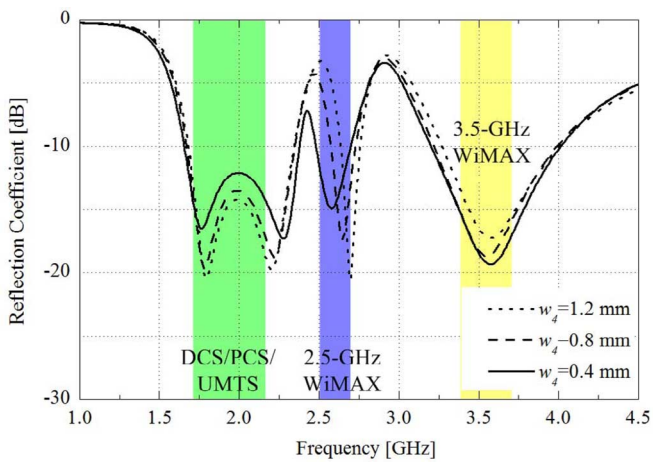

Fig. 9. Simulated S11 of the proposed antenna with different w_4.

three frequencies are 1.05 dB, 0.55 dB, and 0.89 dB, which are listed in Table II. The results illustrate good omnidirectional performance of the proposed antenna.

C. Parameter Study

In this section, key parameters are studied to validate the design strategy. As mentioned above, w_4 is an important parameter for impedance matching. As shown in Fig. 9, with the decrease of w_4, the length of Slot3 increases with the middle frequency band shifting lower. The bandwidths of the lower and higher frequency bands are wider. However, small value for w_4 will be affected by the fabrication error. Therefore, 0.4 mm is chosen for this reason.

The values of l_3 and l_4 are also very sensitive to the frequency response of the proposed antenna. Fig. 10 shows the simulated reflection coefficients of the proposed antenna with different l_3. The variation of l_3 leads to different width of the parasitic loop

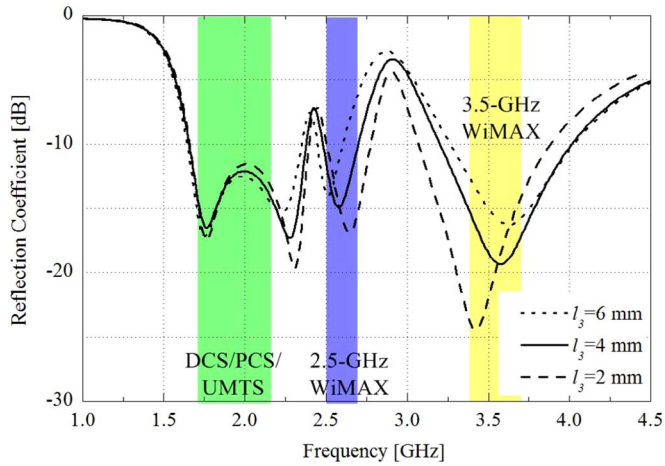

Fig. 10. Simulated S11 of the proposed antenna with different l_3.

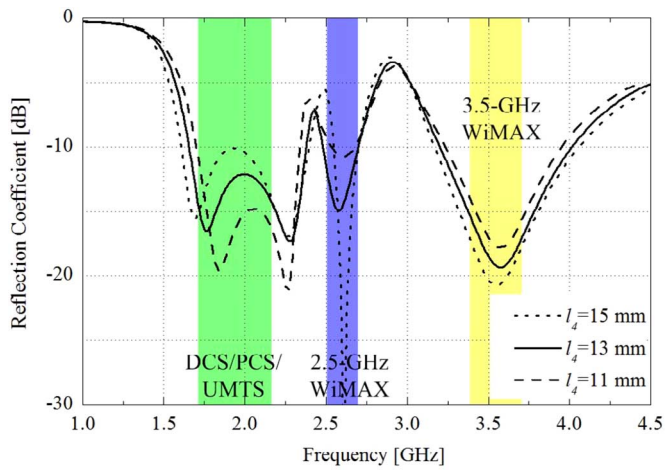

Fig. 11. Simulated S11 of the proposed antenna with different l_4.

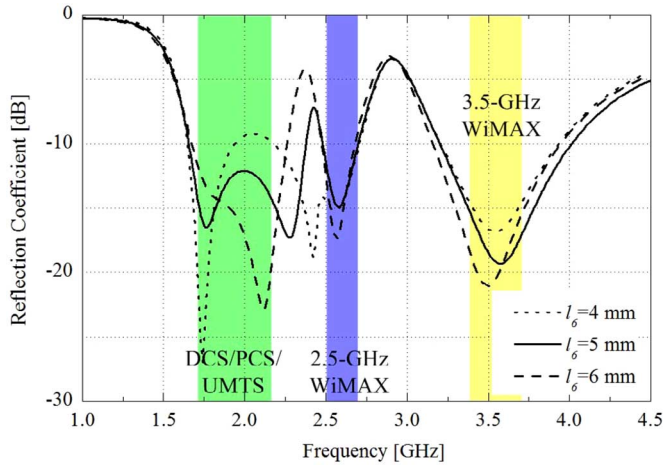

Fig. 12. Simulated S11 of the proposed antenna with different l_6.

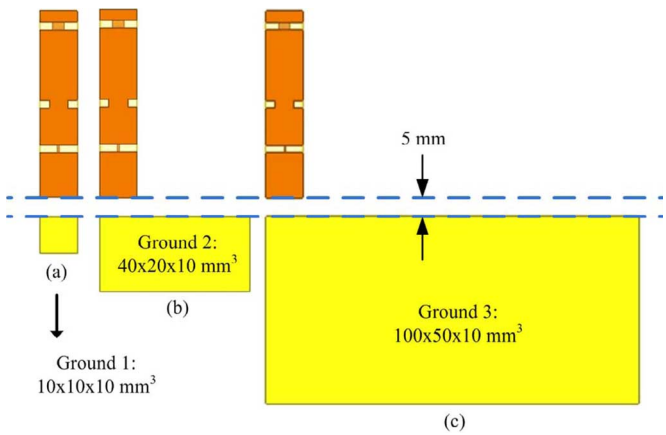

Fig. 13. Antenna application with the additional ground (equipment) with different ground dimension.

ring, which affects the resonant frequency of the higher band. With the decrease of l_3, the resonant frequency of the middle and higher bands shift closer. The bandwidth of lower band is wider. In order to tuning the ratio between the different frequency bands, $l_3 = 4$ mm is selected.

Fig. 11 shows the simulated reflection coefficients of the proposed antenna with different l_4. Due to the DGS effect, l_4 is sensitive to the impedance matching for all the frequency bands. With the increase of l_4, the dual peaks in lower band shift further from each other. The bandwidth of higher band is enhanced. The value of l_4 is also related to the impedance matching of middle band. For the comprehensive consideration, $l_4 = 13$ mm is selected.

Fig. 12 shows the simulated reflection coefficients of the proposed antenna with different l_6. The length of the microstrip line is another important parameter for impedance matching, especially for the lower band. By tuning l_6, dual-resonant with wide impedance bandwidth is achieved. We select $l_6 = 5$ mm, and the lower band covers the DCS, PCS, and UNTS bands.

The shorting positions of the triple slots are discussed here. The Slot1 is directly fed through the microstrip line on Side4. The shorting position of Slot1 is selected on Side2. Slot3 is adopted for DGS impedance matching, and its shorting position is selected on the same side of the microstrip line. Slot2 is fed by coupling current on the column, indirectly by the microstrip line. Therefore, the shorting position of Slot2 can be selected on Side2 or Side4 with identical radiating pattern and impedance bandwidth.

D. Ground Effect Analysis

As discussed in the introduction, the proposed antenna is employed without using large ground. In order to validate this assumption and further emphasize this advantage, the proposed antenna was simulated with different ground plane dimensions. As shown in Fig. 13, the proposed antenna is mounted on different metal boxes (e.g., main body of nearby equipment) with a distance of 5 mm. Three different dimensions of the metal boxes are used here: ground 1 ($10 \times 10 \times 10$ mm^3) in Fig. 13(a), ground 2 ($40 \times 20 \times 10$ mm^3) in Fig. 13(b) and ground 3 ($100 \times 50 \times 10$ mm^3) in Fig. 13(c).

Fig. 14 shows the simulated reflection coefficients of the proposed antenna when placed near metal boxes of different dimensions. As it may be seen, the performance of the proposed antenna continued to be acceptable (i.e., maintained excellent penta-band coverage) even with the presence of nearby metal equipment. The monopole antenna in [8]–[10], on the other hand, cannot operate without a large ground, especially for the situation of ground 1 in Fig. 13(a). The proposed antenna can

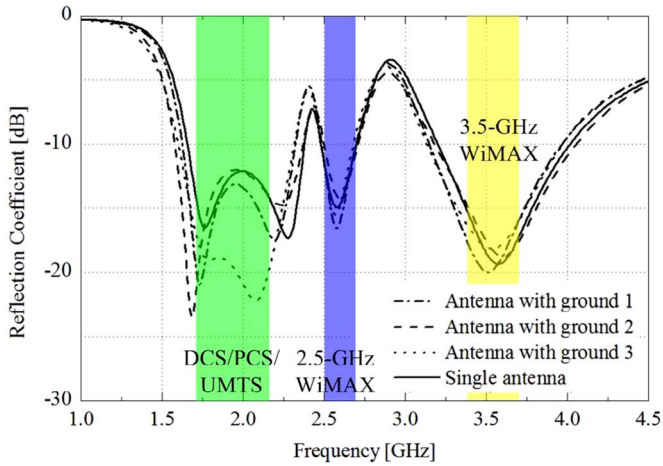

Fig. 14. Simulated S11 of the proposed antenna with different additional ground (equipment).

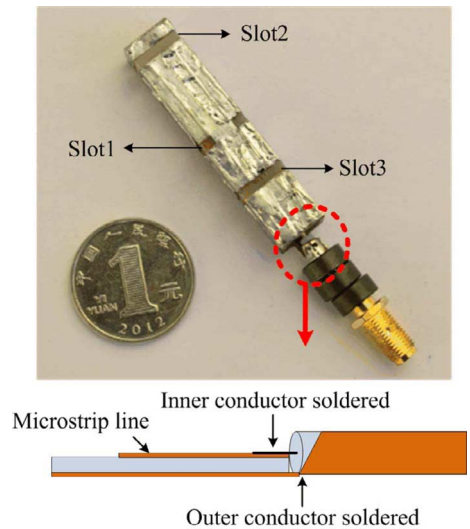

Fig. 15. Photograph of the proposed antenna.

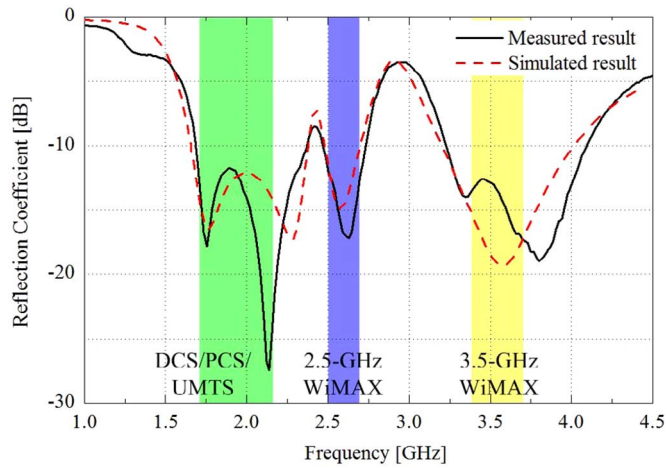

Fig. 16. Measured and simulated S11 of the proposed antenna.

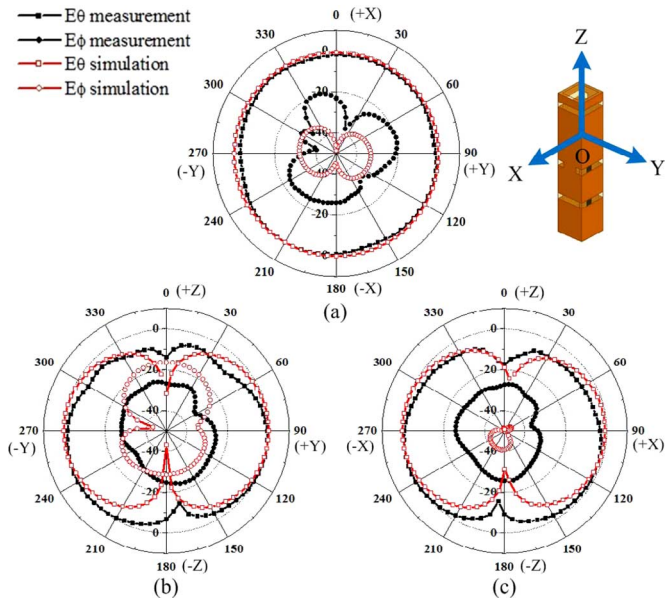

Fig. 17. Simulated and measured normalized radiation patterns of the proposed antenna at 2 GHz. (a) XY-plane; (b) YZ-plane; (c) XZ-plane.

be designed separately without considering the dimensions of associated transmitting or receiving equipment.

III. Experimental Results

In order to prove the design strategy, a prototype of the proposed antenna was built and measured, as shown in Fig. 15. The antenna prototype consists of four printed circuit boards (PCBs), and the seams between four PCBs are covered using foil. Folding the soft PCB is also an acceptable way to build the antenna. The antenna prototype was fed by 50-Ω coaxial cables. As we know, the feeding coaxial cables can be treated as an extension of the metal ground. To avoid the radiating of the current along the feeding coaxial cables, a series of magnetic beads are used to choke the surface current on the feeding cables. The detailed connection figure is also shown in Fig. 15. The inner conductor of the coaxial cable is soldered with the feeding microstrip line. The outer conductor is soldered with the metal on Side4.

The measured results of reflection coefficient are illustrated in Fig. 16, and compared with the simulated results. The -10 dB bandwidths of the reflection coefficient are 1.69–2.37 GHz for the lower band, 2.47–2.72 GHz for the middle band and 3.23–4.09 GHz for the higher band. Once again, wide bandwidth is achieved in a small volume of $50 \times 10 \times 10$ mm^3 ($0.285\lambda_0 \times 0.057\lambda_0 \times 0.057\lambda_0$, λ_0 is the wavelength in free space at 1.71 GHz), without using extra ground.

The measured normalized radiation patterns at 2 GHz, 2.6 GHz, and 3.5 GHz are shown in Figs. 17, 18, and 19, also compared with the simulated results. It is clearly seen that the omnidirectional radiation patterns are achieved for co-polarization in the azimuthal plane (XY-plane) at all the three frequencies, and agree well with the simulated ones. In XZ-plane and YZ-plane, the radiation patterns are nearly "∞"shaped with the nulls at $\pm$Z axis. Due to the undesired radiation and reflection from the feeding cables, the cross-polarization level is higher than the simulated results. The difference between simulation and measurement is acceptable, given the small values of the cross-polarization powers.

Fig. 20 shows the measured gain of the proposed antenna in the azimuthal plane, and compared with the simulation results. In the band of DCS, PCS, and UMTS, the measured gain fluctuates between 1.95 dBi and 2.55 dBi. In the band of 2.5-GHz

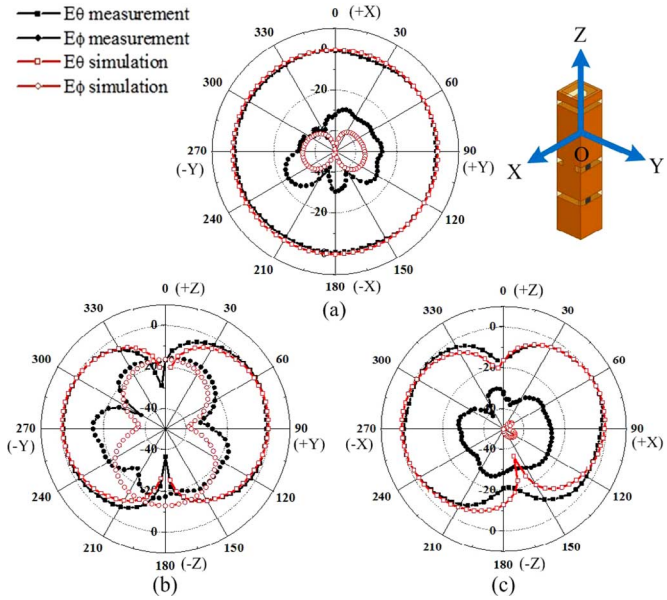

Fig. 18. Simulated and measured normalized radiation patterns of the proposed antenna at 2.6 GHz. (a) XY-plane; (b) YZ-plane; (c) XZ-plane.

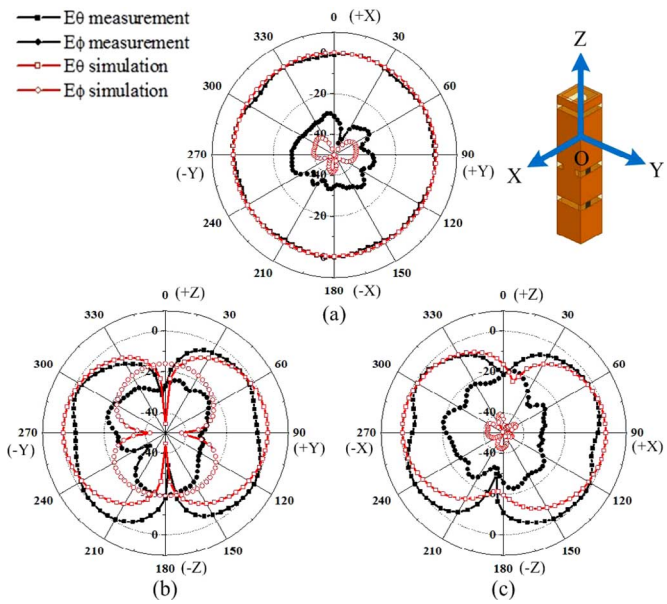

Fig. 19. Simulated and measured normalized radiation patterns of the proposed antenna at 3.5 GHz. (a) XY-plane; (b) YZ-plane; (c) XZ-plane.

WiMAX, the measured gain fluctuates between 0.7 dBi and 1.12 dBi. In the band of 3.5-GHz WiMAX, the measured gain fluctuates between 2.6 dBi and 2.64 dBi. The results are acceptable for practical applications.

IV. Conclusion

This paper proposed a penta-band omnidirectional antenna using three co-located slots on a square columnar structure. The slots not only play the roles of radiating elements, but also serve as the defected ground for impedance matching. The proposed antenna is able to cover five bands, including the bands of DCS, PCS, UMTS, 2.5-GHz WiMAX, and 3.5-GHz WiMAX. The omnidirectional radiation patterns are achieved in the azimuthal plane for all the operating bands, due to the compact square columnar structure. The overall volume of the proposed antenna is only $50 \times 10 \times 10$ mm^3, which is suited for the volume-limited systems. The measured gains of each operating bands are also acceptable for the application in the portable base stations and access points.

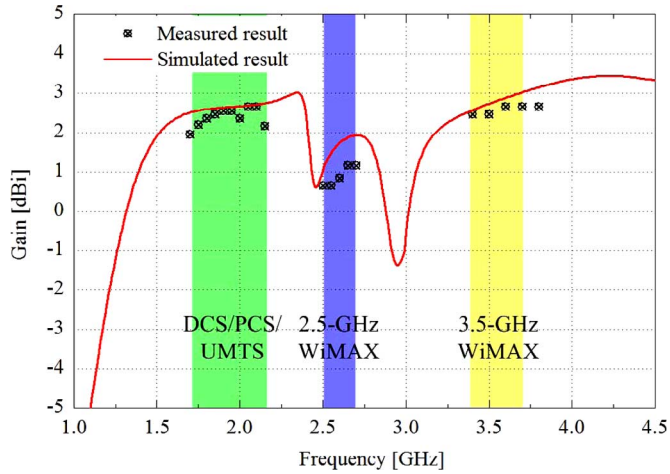

Fig. 20. Simulated and measured gains of the proposed antenna.

Acknowledgment

The authors would like to thank C. Deng and G. Pan from the Department of Electronic Engineering, Tsinghua University, for their help, particularly with antenna fabrication and measurements. They would like to thank the reviewers for their comments and suggestions, which are valuable in improving the paper and also important for our future research.

References

[1] Q. Chu and L. Ye, "Design of compact dual-wideband antenna with assembled monopoles," *IEEE Trans. Antennas Propag.*, vol. 58, no. 12, pp. 4063–4066, Dec. 2010.

[2] W. Liu, C. Wu, and Y. Dai, "Design of triple-frequency microstrip-fed monopole antenna using defected ground structure," *IEEE Trans. Antennas Propag.*, vol. 59, no. 7, pp. 2457–2463, Jul. 2011.

[3] C. Pan, T. Horng, W. Chen, and C. Huang, "Dual wideband printed monopole antenna for WLAN/WiMAX applications," *IEEE Antennas Wireless Propag. Lett.*, vol. 6, pp. 149–151, 2007.

[4] W. Liu, C. Wu, and Y. Tseng, "Parasitically loaded CPW-fed monopole antenna for broadband operation," *IEEE Trans. Antennas Propag.*, vol. 59, no. 6, pp. 2415–2419, Jun. 2011.

[5] S. Palud, F. Colombel, M. Himdi, and C. Meins, "Wideband omnidirectional and compact antenna for VHF/UHF band," *IEEE Antennas Wireless Propag. Lett.*, vol. 10, pp. 3–6, 2011.

[6] R. Zaker and A. Abdipour, "A very compact ultrawideband printed omnidirectional monopole antenna," *IEEE Antennas Wireless Propag. Lett.*, vol. 9, pp. 471–473, 2010.

[7] C. Tseng and C. Huang, "A wideband cross monopole antenna," *IEEE Trans. Antennas Propag.*, vol. 57, no. 8, pp. 2464–2468, Jun. 2009.

[8] K. Wong and C. Wu, "Wide-band omnidirectional square cylindrical metal-plate monopole antenna," *IEEE Trans. Antennas Propag.*, vol. 53, no. 8, pp. 2758–2761, Jun. 2005.

[9] K. Wong, S. Su, and C. Tang, "Broadband omnidirectional metal-plate monopole antenna," *IEEE Trans. Antennas Propag.*, vol. 53, no. 1, pp. 581–583, Jan. 2005.

[10] X. Wu and A. Kishk, "Study of an ultrawideband omnidirectional rolled monopole antenna with trapezoidal cuts," *IEEE Trans. Antennas Propag.*, vol. 56, no. 1, pp. 259–263, Jan. 2008.

[11] R. Bancroft and B. Bateman, "An omnidirectional planar microstrip antenna," *IEEE Trans. Antennas Propag.*, vol. 52, no. 7, pp. 3151–3153, Jul. 2004.

[12] F. Hsiao and K. Wong, "Omnidirectional planar folded dipole antenna," *IEEE Trans. Antennas Propag.*, vol. 52, no. 2, pp. 1898–1902, Feb. 2004.
[13] K. Wei, Z. Zhang, W. Chen, Z. Feng, and M. Iskander, "A triband shunt-fed omnidirectional planar dipole array," *IEEE Antennas Wireless Propag. Lett.*, vol. 9, pp. 850–853, 2010.
[14] J. Li, "An omnidirectional microstrip antenna for WiMAX applications," *IEEE Antennas Wireless Propag. Lett.*, vol. 10, pp. 167–169, 2011.
[15] H. Chreim, E. Pointereau, B. Jecko, and P. Dufrane, "Omnidirectional electromagnetic band gap antenna for base station applications," *IEEE Antennas Wireless Propag. Lett.*, vol. 6, pp. 499–502, 2007.
[16] E. Pointereau, H. Chreim, B. Jecko, and P. Dufrane, "Omnidirectional cylindrical electromagnetic bandgap antenna with dual polarization," *IEEE Antennas Wireless Propag. Lett.*, vol. 6, pp. 450–453, 2007.
[17] A. Borja, P. Hall, Q. Liu, and H. Iizuka, "Omnidirectional loop antenna with left-handed loading," *IEEE Antennas Wireless Propag. Lett.*, vol. 6, pp. 495–498, 2007.
[18] J. Zhu, M. Antoniades, and G. Eleftheriades, "A compact tri-band monopole antenna with single-cell metamaterial loading," *IEEE Trans. Antennas Propag.*, vol. 58, no. 4, pp. 1031–1038, Feb. 2010.
[19] R. Isom, M. Iskander, Z. Yun, and Z. Zhang, "Design and development of multiband coaxial continuous transverse stub (CTS) antenna arrays," *IEEE Trans. Antennas Propag.*, vol. 52, no. 8, pp. 2180–2184, Aug. 2004.
[20] C. Ahn, S. Oh, and K. Chang, "A dual-frequency omnidirectional antenna for polarization diversity of MIMO and wireless communication applications," *IEEE Antennas Wireless Propag. Lett.*, vol. 8, pp. 996–999, 2009.
[21] G. Shiroma and W. Shiroma, "A two-element L-band Quasi-Yagi antenna array with omnidirectional coverage," *IEEE Trans. Antennas Propag.*, vol. 55, no. 12, pp. 3713–3716, Dec. 2007.
[22] M. Wong, A. Sebak, and T. Denidni, "Analysis of a dual-band dual slot omnidirectional stripline antenna," *IEEE Antennas Wireless Propag. Lett.*, vol. 6, pp. 199–202, 2007.

Yue Li (S'11–M'12) received the B.S. degrees in telecommunication engineering from the Zhejiang University, Zhejiang, China, in 2007, and the Ph.D. degree from Tsinghua University, Beijing, China, in 2012.

Since 2012, he has been with Tsinghua University, where he is a Postdoctoral Fellow in the Department of Electronic Engineering. His current research interests include reconfigurable antennas, electrically small antennas, mobile antennas, diversity antennas, and antennas in package. He is a reviewer of the IEEE TRANSACTIONS ON ANTENNAS AND PROPAGATION and the IEEE ANTENNAS AND WIRELESS PROPAGATION LETTERS.

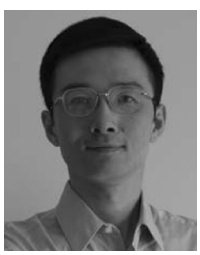

Zhijun Zhang (M'00–SM'04) received the B.S. and M.S. degrees from the University of Electronic Science and Technology of China, in 1992 and 1995, respectively, and the Ph.D. degree from Tsinghua University, Beijing, China, in 1999.

In 1999, he was a Postdoctoral Fellow with the Department of Electrical Engineering, University of Utah, Salt Lake City, UT, USA, where he was appointed a Research Assistant Professor in 2001. In May 2002, he was an Assistant Researcher with the University of Hawaii at Manoa, Honolulu, HI, USA. In November 2002, he joined Amphenol T&M Antennas, Vernon Hills, IL, USA, as a Senior Staff Antenna Development Engineer and was then promoted to the position of Antenna Engineer Manager. In 2004, he joined Nokia Inc., San Diego, CA, USA, as a Senior Antenna Design Engineer. In 2006, he joined Apple Inc., Cupertino, CA, USA, as a Senior Antenna Design Engineer and was then promoted to the position of Principal Antenna Engineer. Since August 2007, he has been with Tsinghua University, China, where he is a Professor in the Department of Electronic Engineering. He is the author of *Antenna Design for Mobile Devices* (Wiley, 2011). He is an Associate Editor of the IEEE TRANSACTIONS ON ANTENNAS AND PROPAGATION and the IEEE ANTENNAS AND WIRELESS PROPAGATION LETTERS.

Zhenghe Feng (M'05–SM'08–F'12) received the B.S. degree in radio and electronics from Tsinghua University, Beijing, China, in 1970.

Since 1970, he has been with Tsinghua University, China, as an Assistant, Lecturer, Associate Professor, and Full Professor. His main research areas include numerical techniques and computational electromagnetics, RF and microwave circuits and antennas, wireless communications, smart antennas, and spatial temporal signal processing.

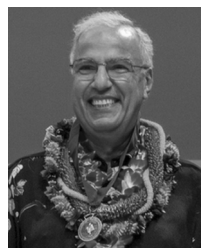

Magdy F. Iskander (S'72–M'76–SM'84–F'93–LF'12) is the Director of the Hawaii Center for Advanced Communications (HCAC), College of Engineering, University of Hawaii at Manoa, Honolulu, HI, USA. He is Co-Director the NSF Industry/University Cooperative Research Center with four other universities.

From 1997–1999, he was a Program Director at the National Science Foundation, where he formulated a "Wireless Information Technology" Initiative in the Engineering Directorate. He edited two special issues of the IEEE TRANSACTIONS ON ANTENNAS AND PROPAGATION on Wireless Communications Technology in 2002 and 2006 and co-edited a special issue of the *IEICE Journal* in Japan in 2004. He was the 2002 President of IEEE Antennas and Propagation Society (AP-S) and a Distinguished Lecturer for the IEEE AP-S (1994–1997). He authored the textbook *Electromagnetic Fields and Waves* (Prentice Hall, 1992, and Waveland Press, 2001; second edition 2012); edited the *CAEME Software Books*, Vol. I, II 1991–94; and edited four books on *Microwave Processing of Materials* (Materials Research Society, 1990–1996). He has published over 230 papers in technical journals, holds eight patents, and has made numerous presentations at national and international conferences. He is the founding editor of the *Computer Applications in Engineering Education* (CAE) journal, published by Wiley (1992–present). Much of his research is funded by the National Science Foundation, the U.S. Army CERDEC, and the Office of Naval Research, as well as several corporate sponsors. As a result of an NSF Major Research Instrumentation grant, he established wireless testbeds, indoor antenna ranges, microwave network analysis labs, and an RF fabrication and characterization lab at the University of Hawaii at Manoa. His Center HCAC has an ongoing ten-year grant (2005–2014) for partnership in the NSF Industry/University Cooperative Research Center in Telecommunications with the University of Arizona, Arizona State University, RPI, and The Ohio State University. His research focus is on antenna design and propagation modeling for wireless communications and radar systems and his group recently received two NSF grants and CERDEC funding for the development of the "Microwave Stethoscope" for vital signs and changes in lung water content measurement.

Dr. Iskander has received many teaching excellence and research awards, including the 2012 University of Hawaii Board of Regent Medal for Excellence in Research and the 2010 Board of Regents' Medal for Teaching Excellence. In 2012, he received the IEEE AP-S Chen-To Tai Distinguished Educator Award and the 2013 IEEE MTT-S Distinguished Educator Award. He also received the 2010 Northrop Grumman Excellence in Teaching Award, the 2011 Hi Chang Chai Outstanding Teaching Award, and the University of Utah Distinguished Teaching Award in 2000. In 1985, he received the ASEE Curtis W. McGraw National Research Award, and in 1991, he received the ASEE George Westinghouse National Education Award. 1992, he also received the Richard R. Stoddard Award from the IEEE EMC Society. He was a member of the 1999 WTEC panel on "Wireless Information Technology-Europe and Japan", and chaired two International Technology Institute Panels on "Asian Telecommunication Technology" sponsored by NSF/DoD in 2001 and 2003.